AGU PUBLICATIONS

JGR

Journal of Geophysical Research: Biogeosciences

RESEARCH ARTICLE
10.1002/2016JG003347

Key Points:
- Microbial phospholipids examined along grassland to woodland chronosequence
- Increase in gram-negative bacteria (cy19:0) with stand age
- Microbes predominately assimilate accessible woodland C

Supporting Information:
- Supporting Information S1
- Data Set S1
- Data Set S2
- Data Set S3
- Data Set S4

Correspondence to:
C. A. Creamer,
courtneycreamer@gmail.com

Citation:
Creamer, C. A., T. R. Filley, T. W. Boutton, and H. I. Rowe (2016), Grassland to woodland transitions: Dynamic response of microbial community structure and carbon use patterns, *J. Geophys. Res. Biogeosci.*, *121*, 1675–1688, doi:10.1002/2016JG003347.

Received 22 JAN 2016
Accepted 7 JUN 2016
Accepted article online 13 JUN 2016
Published online 28 JUN 2016

©2016. American Geophysical Union. All Rights Reserved.

Grassland to woodland transitions: Dynamic response of microbial community structure and carbon use patterns

Courtney A. Creamer[1], Timothy R. Filley[1], Thomas W. Boutton[2], and Helen I. Rowe[3,4]

[1]Department of Earth and Atmospheric Sciences and Purdue Climate Change Research Center, Purdue University, West Lafayette, Indiana, USA, [2]Department of Ecosystem Science and Management, Texas A&M University, College Station, Texas, USA, [3]McDowell Sonoran Conservancy, Scottsdale, Arizona, USA, [4]School of Life Sciences and Julie Ann Wrigley Global Institute of Sustainability, Arizona State University, Tempe, Arizona, USA

Abstract Woodland encroachment into grasslands is a globally pervasive phenomenon attributed to land use change, fire suppression, and climate change. This vegetation shift impacts ecosystem services such as ground water allocation, carbon (C) and nutrient status of soils, aboveground and belowground biodiversity, and soil structure. We hypothesized that woodland encroachment would alter microbial community structure and function and would be related to patterns in soil C accumulation. To address this hypothesis, we measured the composition and $\delta^{13}C$ values of soil microbial phospholipids (PLFAs) along successional chronosequences from C_4-dominated grasslands to C_3-dominated woodlands (small discrete clusters and larger groves) spanning up to 134 years. Woodland development increased microbial biomass, soil C and nitrogen (N) concentrations, and altered microbial community composition. The relative abundance of gram-negative bacteria (cy19:0) increased linearly with stand age, consistent with decreases in soil pH and/or greater rhizosphere development and corresponding increases in C inputs. $\delta^{13}C$ values of all PLFAs decreased with time following woody encroachment, indicating assimilation of woodland C sources. Among the microbial groups, fungi and actinobacteria in woodland soils selectively assimilated grassland C to a greater extent than its contribution to bulk soil. Between the two woodland types, microbes in the groves incorporated relatively more of the relict C_4-C than those in the clusters, potentially due to differences in below ground plant C allocation and organo-mineral association. Changes in plant productivity and C accessibility (rather than C chemistry) dictated microbial C utilization in this system in response to shrub encroachment.

1. Introduction

Woody plant encroachment into grass-dominated ecosystems is a globally pervasive land cover change that alters aboveground and belowground C storage and cycling rates [*Jackson et al.*, 2002; *Boutton et al.*, 2009; *Barger et al.*, 2011; *Blaser et al.*, 2014; *Saintilan and Rogers*, 2015]. This important vegetation change is driven by several phenomena, including reduced fire frequencies, chronic livestock grazing, and rising atmospheric CO_2 concentrations [*Scholes and Archer*, 1997; *Bond and Midgley*, 2000; *Knapp et al.*, 2008; *de Graaff et al.*, 2014]. As both increases and decreases in soil organic C (SOC) and N have been observed in response to woody encroachment [*Jackson et al.*, 2002; *Eldridge et al.*, 2011], this widespread land cover change represents an uncertainty in global C cycling models [*Pacala et al.*, 2001; *Barger et al.*, 2011]. Identifying relevant environmental drivers of soil organic matter (SOM) stability, particularly the importance of microbial community composition and activity, may help reduce the uncertainty in predicting changes in soil C with woodland encroachment.

In the Rio Grande Plains region of southern Texas, C_3 woody plants have been encroaching into C_4-dominated grasslands over the past 150 year [*Archer*, 1990]. This land cover shift is associated with greater aboveground and belowground plant productivity and higher soil C and N concentrations [*Archer et al.*, 2001; *Hibbard et al.*, 2001, 2003]. The chemistry and physical accessibility of SOC has also changed with woodland encroachment in this region, with increases in rapidly cycled, physically accessible soil fractions, but also increases in more structurally complex polymers that may have slower turnover [*Liao et al.*, 2006a, 2006b; *Filley et al.*, 2008]. These decreases in physical protection of SOM (i.e., accessibility) but increases in chemical complexity along with higher rates of C inputs have impacted microbial activity, resulting in

overall increases in C and N cycling, but at a rate that does not keep pace with the accumulation of soil C and N. For example, although total microbial biomass and C mineralization is higher in the woodlands, microbial biomass and respiration per unit of SOC decreases, suggesting the community is less efficient at processing C inputs [*McCulley et al*., 2004; *Liao and Boutton*, 2008]. Similarly, measured decreases in N enzyme activity (per unit soil N) for protein and amino sugar acquisition suggest the woodland microbial community is less efficient at processing accumulated soil N [*Creamer et al*., 2013a]. Although there is preliminary evidence that microbial community composition is altered by woodland encroachment [*Brewer*, 2010; *Kantola*, 2012], it remains unclear whether these potential changes have impacted biogeochemical processes in this ecosystem.

The primary aim of this study was to determine whether changes in microbial community composition and function are contributing to changes in SOM stocks with woody encroachment in southern Texas by addressing the following questions: (1) how does microbial community composition and SOC assimilation respond to altered plant inputs and (2) do broad microbial groups respond differently to changes in C source composition? Changes in C source assimilation between microbial groups in the grasslands and the woodlands would suggest changes in the function of particular microbial groups, potentially resulting from changes in plant input chemistry. We hypothesized that fungi would increase in relative abundance and preferentially utilize woodland C, due to increases in chemically complex woody debris and root biomass with woody encroachment [*Hibbard et al*., 2001], and the association of fungi with the decomposition of both wood [*Blanchette*, 1991; *Brant et al*., 2006] and fresh plant inputs [*Butler et al*., 2003; *Amelung et al*., 2008; *Tavi et al*., 2013]. We also expected gram-negative bacteria to increase in relative abundance and woodland C utilization due to their association with the rhizosphere [*Treonis et al*., 2004], as this is demonstrated to expand in the woodland areas [*Hibbard et al*., 2001]. Finally, we predicted that gram-positive bacteria would decrease in relative abundance and preferentially utilize grassland C, due to their association with SOM decomposition [*Kramer and Gleixner*, 2006, 2008]. In sum, changes in microbial community composition and function would reflect not only the increasing chemical complexity but also the increasing quantity of C inputs with woodland encroachment.

2. Materials and Methods

2.1. Site Description

Soils were sampled from the Texas A&M AgriLife La Copita Research Area (27°40′N; 98°12′W) in the Rio Grande Plains region of southern Texas. Upland soils are generally Typic Argiustolls with a sandy loam surface and an argillic horizon at 40–60 cm; however, patches of Typic Haplustepts lacking an argillic horizon are also included in the uplands. Upland portions of the landscape have a grassland matrix dominated by C_4 grass species (*Chloris cucullata*, *Tridens muticus*, *Bouteloua* sp., *Aristida purpurea*, *Panicum hallii*, and *Eragrostis* sp.) as well as C_3 forbs (*Wedelia hispida*, *Ambrosia psilostachya*, and *Gutierrezia* sp.). Within this grassland matrix, discrete woody clusters (<10 m diameter) have developed. Where the argillic horizon is absent, these woody clusters often expand and fuse to form larger (10–100 m diameter) woody groves [*Archer et al*., 1995; *Bai et al*., 2012]. Individual clusters and groves generally include approximately 10–30 C_3 tree and shrub species and are dominated by *Prosopis glandulosa*, *Zanthoxylum fagara*, *Celtis pallida*, *Condalia hookeri*, *Zizyphus obtusifolia*, and *Diospyros texana*. The $\delta^{13}C$ values of grassland SOC reflect a mix of C_3 and C_4 inputs (about −19‰), while those of clusters and groves reflect the woodland C_3 inputs, with values ranging from −20 to −26‰ [*Boutton et al*., 1998; *Bai et al*., 2009].

2.2. Soil Sampling

Soil cores (0–5 cm deep × 5 cm diameter) were taken on 14–16 May 2007 and on 19 October 2007 from 15 remnant grassland sites, 15 discrete woody cluster sites, and 15 grove sites. Surface litter was gently removed (with minimal disturbance to the mineral soil) prior to soil sampling. Cores from clusters and groves were taken in the four cardinal directions within 50 cm of the base of the largest mesquite tree. Cluster tree ages ranged from 14 to 86 years with an average age of 50.3 years; grove tree ages ranged from 16 to 134 years with an average age of 67.6 years. Woody cluster and grove tree ages were determined using regression equations [*Stoker*, 1997] that predict tree age from the basal diameter of the mesquite tree. The 15 grassland soils were sampled in the four cardinal directions around a randomly selected C_4 grass at least 3 m from the

edge of each of the woody cluster canopies. After sampling, all cores were put on ice and stored at −20°C until further processing.

2.3. Analytical Procedures

2.3.1. Phospholipid Extraction, Quantification, and $\delta^{13}C$ Measurements

The four frozen soil cores from each cluster, grove, and associated grass were combined, freeze-dried, and sieved to <2 mm. Large roots (>2 mm diameter) were removed and phospholipids (PLFAs) were extracted from 5 g subsamples as outlined by *Bligh and Dyer* [1959] and modified by *White et al*. [1979] and *Findlay et al*. [1989]. Briefly, lipids were extracted overnight in chloroform, methanol, and phosphate buffer; phospholipids were isolated by solid phase extraction and dried under a stream of N_2 (see supporting information for further details). PLFAs were resuspended in 1 mL chloroform, and two 100 μL splits were taken, one for phosphate-biomass measurements (see below) and the other for quantification of fatty acid methyl esters (FAMEs) by gas chromatography-mass spectrometry (GC-MS; described in supporting information). The remaining 800 μL were used to determine the $\delta^{13}C$ values of FAMEs by compound specific gas chromatography-combustion-isotope ratio mass spectrometry (GC-C-IRMS; described in supporting information).

Microbial biomass was quantified by the phosphate content liberated from extracted phospholipids with potassium persulfate digestion and absorbance at 610 nm after addition of a malachite green-oxalate salt dye [*Findlay et al*., 1989]. A conversion factor of 340 μmoles lipid phosphate g^{-1} biomass C was used to convert microbial phosphate to microbial biomass C [*Frostegård et al*., 1991]. This method produced comparable results to the sum of all PLFAs quantified by GC-MS (data are not shown).

2.3.2. Soil C, N, and $\delta^{13}C$ Measurements

Subsamples of the <2 mm sieved freeze-dried soils used for phospholipid extractions were ground to a fine powder using a steel ball mill (Retsch, Haan, Germany). Concentrations of SOC and total N and $\delta^{13}C$ values of SOC were measured in duplicate on the ground soils using a CHN elemental analyzer (Sercon Ltd., Crewe, UK) interfaced to the 20/22 IRMS. $\delta^{13}C$ values are expressed relative to the international Vienna Pee Dee Belemnite (VPDB) standard [*Coplen*, 2011]. Analytical precision of $\delta^{13}C$ of the internal isotopic standard (Standard Reference Material 1547 Peach Leaves, NIST, Gaithersburg, MD) was 0.2‰.

2.4. Calculations and Statistics

2.4.1. Mass Balance and Turnover Rates From Isotopes

First-order exponential rise to maximum models were fit to the increase in SOC and total N concentrations in relation to grove and cluster stand age in SigmaPlot (v12.3):

$$y(t) = y_0 + a\left(1 - e^{-kt}\right), \tag{1}$$

where $y(t)$ is C or N concentration (mg kg $soil^{-1}$) at a stand age of t years, y_0 is the y intercept at t of 0 year, and a is the maximum C (or N) concentration with a rate constant of k ($year^{-1}$). The exponential decay form of equation (1) was fit to decreasing $\delta^{13}C$ values of SOC and PLFA relative to stand age. In some instances a linear regression model ($y[t] = mt + b$) was used if it provided a better fit.

The measured isotopic composition of individual PLFAs was corrected for the contribution of the methyl carbon added to FAMEs during methylation. This was determined using the following equation:

$$\delta^{13}C_{PLFA} = \frac{\left(\delta^{13}C_{FAME} \times N\right) - \delta^{13}C_{MEOH}}{(N-1)}, \tag{2}$$

where $\delta^{13}C_{PLFA}$ is the isotopic composition of the individual PLFAs, $\delta^{13}C_{FAME}$ is the isotopic composition of the FAME (measured by GC-C-IRMS), $\delta^{13}C_{MeOH}$ is the isotopic composition of the methanol (−35.1‰; $n = 10$ determined by elemental analysis [EA]-IRMS), and N is the number of carbon atoms in the FAME.

The percentage of grassland-derived SOC (F_G) was calculated using a mixing model [*Balesdent and Mariotti*, 1996]:

$$F_G = \frac{\left(\delta^{13}C_{SOC} - \delta^{13}C_W\right)}{\left(\delta^{13}C_G - \delta^{13}C_W\right)}, \tag{3}$$

where $\delta^{13}C_{SOC}$ is the isotopic composition of SOC, $\delta^{13}C_W$ is the average isotopic composition of C_3 woody plants (−26.9‰), and $\delta^{13}C_G$ is the average isotopic composition of SOC from the grassland (C_4 dominated)

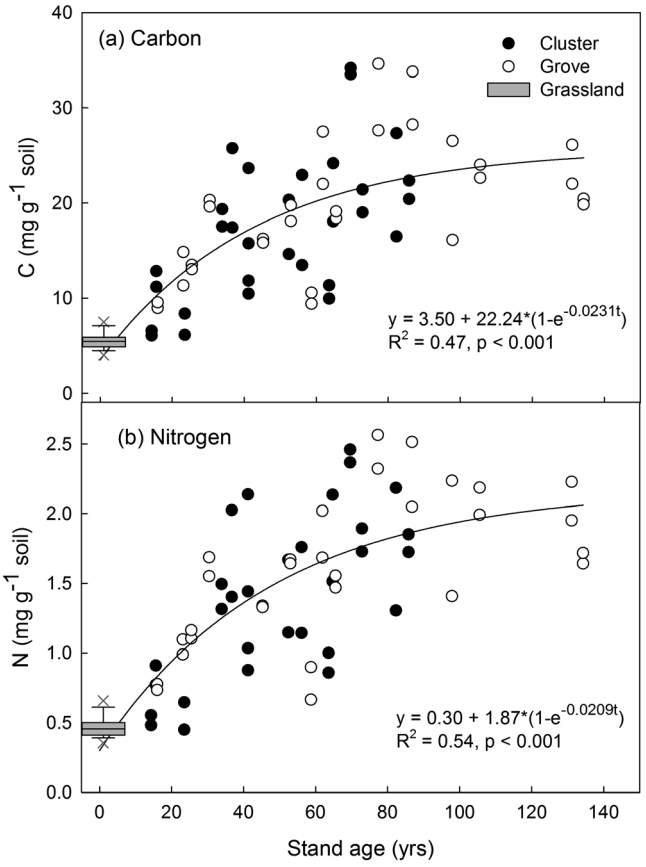

Figure 1. Increases in soil (a) organic carbon and (b) total nitrogen in relation to woodland stand age. Grassland soils are represented by a box plot at time 0 with the whiskers at the 10th and 90th percentiles (box plot outliers shown as an X).

soils (−18.8‰). This mixing model assumes no fractionation between plant source and resulting $\delta^{13}C$ values of SOC. Due to the slight enrichment of ^{13}C during decomposition (typically 1‰) [*Natelhoffer and Fry*, 1988], it may slightly overestimate grassland C. Total SOC yields (mg OC kg^{-1} soil) were then multiplied by F_G to calculate the amount of grassland C (woodland C was calculated as grassland C subtracted from total SOC). The increase in woodland C was fit with the exponential rise-to-maximum equation (equation (1)).

2.5. Statistical Analyses

The yield of individual phospholipids (nmol) was divided by the yield of total phospholipids to obtain relative abundances (mol %). The relative abundances (mol %) of PLFAs were then analyzed with principal component analysis (PCA) using PRIMER (v7). Permutational analysis of variance (PERMANOVA) in PRIMER was used to determine whether there were significant groupings based upon landscape element (grassland, cluster, and grove) or season (May and October). A BEST analysis between stand age and PLFA relative abundances was used to determine which PLFA were most related to stand age; these PLFA were then individually examined with linear regression in SigmaPlot. The trends in $\delta^{13}C$ values of PLFAs relative to SOC and stand age were explored using linear regression and the first-order exponential decay model (equation (1)) in SigmaPlot.

Differences in SOC and total N concentrations, C:N ratios, $\delta^{13}C$ values, microbial biomass yields, average $\delta^{13}C$ values of microbial PLFA ($\delta^{13}C_{PLFA}$), average $\delta^{13}C$ values of PLFAs relative to soil ($\delta^{13}C_{PLFA}$-$\delta^{13}C_{SOIL}$), and relative abundances of PLFAs in microbial groups were analyzed using two-way analysis of variance (ANOVA) in GenStat (sixteenth edition) with sampling season (May and October) and landscape element (grassland, cluster, and grove) as fixed effects and with site as a random effect. In many instances the clusters and groves were not significantly different from one another and data are instead presented for the woodland soils together for brevity. Data were log transformed prior to analysis if it did not meet assumptions of normality (SOC and total N concentrations, C:N ratios). Significant main effects of sampling season or landscape element determined by ANOVA and PERMANOVA are only discussed if interactions between fixed effects were not significant. Significance was set at $\alpha < 0.05$. Values presented in text are averages ± standard errors unless otherwise indicated.

3. Results

3.1. Soil C and N Concentrations and $\delta^{13}C$ Values

The average concentrations of SOC and total *N* in grassland soils (5.5 ± 0.2 and 0.48 ± 0.02 g kg $soil^{-1}$, respectively) were significantly ($P < 0.001$) lower than in woodland soils (18.5 ± 0.9 and 1.51 ± 0.07 g kg $soil^{-1}$). Both

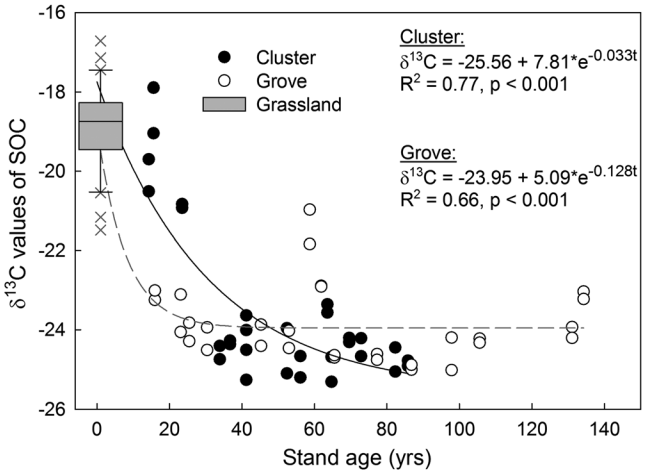

Figure 2. Decrease in $\delta^{13}C$ values of soil organic carbon with increasing woody stand age. Grassland soils are represented by a box plot at time 0 with the whiskers at the 10th and 90th percentiles (box plot outliers shown as an X).

SOC and total *N* increased rapidly with woodland stand age to approximately 80 years, after which increases in C and N began to slow (Figures 1a and 1b). Soil bulk density, while not measured for this study, decreases in the upper 10 cm from approximately 1.18 g cm^{-3} in the grassland soils to 0.90 g cm^{-3} in the cluster soils, with grove soils similar to clusters [*Liao et al.*, 2006a]. Using this range in bulk densities as an approximation for the upper 0–5 cm of soil, C and N increased from roughly 330 g C m^{-2} and 28 g N m^{-2} in the grassland soils to 1100 g C m^{-2} and 92 g N m^{-2} in woodland soils > 80-year of age. The C:N ratio increased significantly from May to October in the grassland soils (10.9 ± 0.1 to 12.4 ± 0.2, respectively) but not in the cluster (12.3 ± 0.2 to 12.6 ± 0.2) or grove soils (12.3 ± 0.1 to 12.2 ± 0.2), so that the C:N ratio of soils in the grasslands was significantly ($P < 0.001$) lower than the woodlands in May but not October.

The $\delta^{13}C$ values of SOC decreased exponentially with stand age reflecting rapid increases of woodland C from litterfall and root turnover and the simultaneous loss of grassland C through decomposition (Figure 2). Consequently, average $\delta^{13}C$ values of SOC under the clusters (−23.5 ± 0.4‰) and groves (−23.9 ± 0.2‰) were significantly lower ($P < 0.001$) than those under the remnant grasslands (−18.9 ± 0.2‰). Replacement of grassland C with woodland C was slightly faster in the groves (*k* of 0.128 $years^{-1}$) relative to the clusters (0.033 $years^{-1}$), although the predicted maximum extent of ^{13}C depletion based upon woody plant $\delta^{13}C$ values was greater in the clusters (−25.6‰) than in the groves (−24.0‰, Figure 2). There was no impact of sampling season on the $\delta^{13}C$ values of SOC. The decrease in soil $\delta^{13}C$ values along with the increase in soil C concentrations with stand age increased woodland C, while grassland C remained relatively constant (Figure 3).

3.2. Microbial Biomass and Community Composition

Microbial biomass C (per kg soil) was significantly ($P < 0.001$) lower in the grassland soils relative to the cluster and grove soils, which were not different from one another (Table 1). However, in the grassland soils

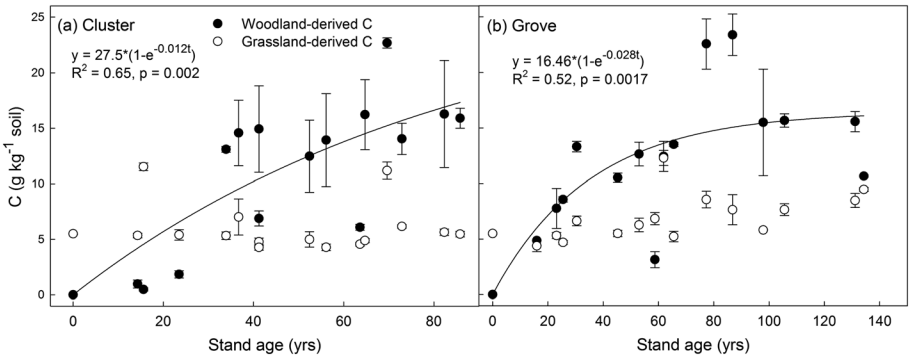

Figure 3. Concentrations of grassland and woodland C in the (a) cluster and (b) grove soils. Error bars represent the average across two seasons. Curve fits for increases in woodland C are shown. Note the difference in *x* axis scales between panels.

Table 1. Microbial Biomass Yields, Per Kilograms of Soil and Soil-C, and the Ratio of Gram-Positive Bacteria to Gram-Negative Bacteria (G+:G−)[a]

	Microbial Biomass C		
Landscape Element	mg kg^{-1} soil	mg g^{-1} soil-C	G+:G−
Grassland	294 ± 36 a	53.8 ± 6.5 a	0.62 ± 0.03 a
Cluster	520 ± 35 b	34.7 ± 3.5 b	0.46 ± 0.01 b
Grove	433 ± 33 b	24.1 ± 2.2 b	0.46 ± 0.01 b

[a]Values are means ± standard errors. Letters indicate significant differences between landscape elements.

microbial biomass per unit of soil C was significantly ($P = 0.005$) higher than in the woodland soils. There was no effect of sampling season on total microbial biomass.

Principle component analysis (PCA) of individual PLFAs revealed differences in microbial community composition with landscape element and season (Figure 4). PLFAs from grassland soils separated from woodland soils along PC1, while PLFAs from May to October were partially separated along PC2. Microbial community composition was significantly different between May and October in the grassland ($P = 0.001$), cluster ($P = 0.002$), and grove ($P = 0.02$) soils. In both seasons, microbial community composition under the grasslands was significantly distinct from both woodlands ($P = 0.001$). However, while communities under the clusters were distinct from the groves in May ($P = 0.006$), in October they were similar ($P = 0.214$). The BEST procedure in PRIMER determined that relative abundances (mol %) of all PLFAs were significantly correlated (rho = 0.40, $P = 0.001$) with woodland age (using age 0 for grassland soils). Cy19:0 showed the strongest relationship to stand age (Figure 5). Relative decreases in 16:0, a17:0, and 10Me18:0 with stand age were significant but much weaker, with respective R^2 values of 0.06, 0.11, and 0.15 and respective P values of 0.049, 0.007, and 0.002 (supporting information Figure S1; no other trends were significant).

These differences in individual PLFAs were reflected in patterns of diagnostic microbial groups (Table 2). Gram-negative bacteria were significantly higher in the woodland soils, while gram-positive bacteria were significantly higher in the grassland soils in October but not May. This resulted in a lower ratio of gram-positive to gram-negative bacteria (G+:G−) in the woodlands relative to the grasslands across both seasons (Table 1) and in May (0.49 ± 0.02) relative to October (0.54 ± 0.02). Fungi decreased significantly from May to October in the grassland and cluster soils, but not in the grove soils, so there were fewer fungi in the groves relative to the clusters in May and more fungi in the groves relative to the grasslands in October. This resulted in seasonal trends in the F:B ratio, with grove soils having a lower F:B ratio in May relative to grasslands and cluster soils, but a higher F:B ratio in October relative to the grassland soils (with clusters intermediate). Actinobacteria increased significantly from the grove to the cluster to the grassland soils and were significantly higher in October (4.7 ± 0.2%) relative to May (4.2 ± 0.1%).

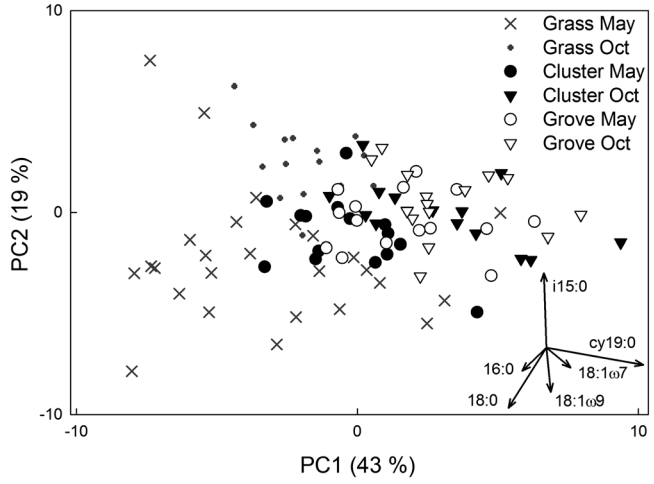

Figure 4. Principal component analysis of the relative abundance (mol %) of PLFAs extracted in the three landscape elements over two seasons. Clusters are filled symbols and groves are open symbols, with sampling season distinguished by circles (May) and triangles (October). Grasslands are indicated by an X (May) or a dot (October). The percentage variance explained by each principal component (PC) is given. PLFAs with correlations > 0.20 along one of the PCs are shown in the lower right-hand corner of the graph; line lengths represent the strength of the loading.

3.3. Microbial Carbon Source Utilization Patterns

The $\delta^{13}C$ value of every measured PLFA was significantly lower in the woodland soils relative to the grassland soils (supporting information Data Set S3). As a result, the average $\delta^{13}C$ value of all microbial lipids (the sum of the relative abundances of individual lipids multiplied by the $\delta^{13}C$ value) increased significantly as follows: clusters < groves < grasslands (Figure 6a). The average $\delta^{13}C$ values of PLFA of microbial groups followed a similar trend. Among

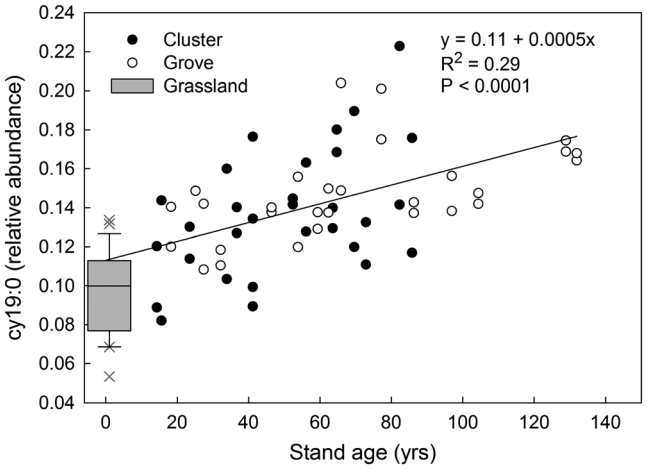

Figure 5. Relative abundance (mol %) of the PLFA cy19:0 with woodland stand age. Grassland soils are represented by a box plot at time 0 with the whiskers at the 10th and 90th percentiles (box plot outliers shown as an X).

individual PLFA, there were significant ($P < 0.0001$) linear relationships between the $\delta^{13}C$ values of PLFA and the $\delta^{13}C$ values of SOC across all landscape elements, explaining 38–72% of the variation in $\delta^{13}C$ values of individual PLFA (supporting information Figure S2).

The correlations between $\delta^{13}C$ values of PLFA and SOC indicate that microbes were generally assimilating C sources consistent with the dominant C source in the bulk soil (i.e., more woodland SOC results in greater woodland C assimilation). However, microbes could show preferences for ^{13}C depleted C (or ^{13}C enriched C) by assimilating these distinct sources to a greater extent than the relative abundance in the bulk soil due to greater proximity, accessibility, or lability. This preference can be determined by comparing the offset between $\delta^{13}C$ values of PLFA and $\delta^{13}C$ values of SOC ($\delta^{13}C_{PLFA}$-$\delta^{13}C_{SOIL}$). Assuming this offset in grassland soils represents isotopic fractionation during PLFA biosynthesis [*Hayes*, 2001] and that the fractionation is the same in the woodland soils, any shift toward more negative $\delta^{13}C_{PLFA}$-$\delta^{13}C_{SOIL}$ values in woodland soils (relative to grassland soils) indicates preferential assimilation of ^{13}C depleted sources (i.e., woodland-derived sources) to an extent greater than woodland C contributions to bulk soil. This trend was observed in total lipids from the cluster soils (Figure 6b). In contrast, a smaller offset between $\delta^{13}C_{PLFA}$-$\delta^{13}C_{SOIL}$ values in woodland soils (relative to grassland soils) indicates greater assimilation of ^{13}C enriched sources (here grassland C) than the contribution to bulk soil. This latter trend was observed in the total PLFA from the grove soils. Fungi and actinobacteria in woodland soils also assimilated slightly more ^{13}C-enriched C sources relative to SOC than those in the grassland soils. Gram-positive and gram-negative bacteria used more ^{13}C-enriched SOC sources in the groves than in the grassland and cluster soils. Among microbial groups, fungal biomass was the most ^{13}C-depleted relative to SOC, while bacterial biomass was the most ^{13}C-enriched.

Table 2. Relative Distribution of Microbial Groups (% of Total PLFAs) and Ratio of Fungi to Bacteria (F:B) Among the Landscape Elements Across Sampling Seasons[a]

	Microbial Groups (% of Total)					
	G+	G−	Actino[b]	Fungi	General[c]	F:B[d]
			May			
Grassland	20.7 ± 1.2 a	37.4 ± 0.7 A	5.2 ± 0.2 A	3.3 ± 0.3 ab	31.2 ± 1.1 a	0.053 ± 0.005 a
Cluster	19.7 ± 0.5 a	43.6 ± 0.5 B	3.9 ± 0.2 B	3.9 ± 0.2 a	26.6 ± 0.7 b	0.058 ± 0.004 a
Grove	20.4 ± 0.6 a	45.1 ± 0.8 B	3.7 ± 0.1 C	2.8 ± 0.2 b	25.8 ± 0.6 b	0.041 ± 0.03 b
			October			
Grassland	25.2 ± 0.6 a*	37.7 ± 0.6	5.8 ± 0.2	2.0 ± 0.1 a*	26.7 ± 0.3 a*	0.030 ± 0.002 a*
Cluster	20.8 ± 0.6 b	44.7 ± 0.9	4.4 ± 0.3	2.5 ± 0.2 ab*	25.2 ± 0.5 ab	0.036 ± 0.003 ab*
Grove	21.1 ± 0.5 b	45.5 ± 0.7	3.9 ± 0.2	3.2 ± 0.3 b	23.7 ± 0.4 b*	0.045 ± 0.005 b

[a]Values are means ± standard errors. Lowercase letters indicate significant differences between landscape elements within a sampling season while asterisks indicate significant differences between sampling season within a landscape element. Capital letters indicate significant differences between landscape elements across seasons.
[b]Actinobacteria.
[c]General microorganisms.
[d]F = 18:2ω6,9c, B = G+, G–, and actinobacteria.

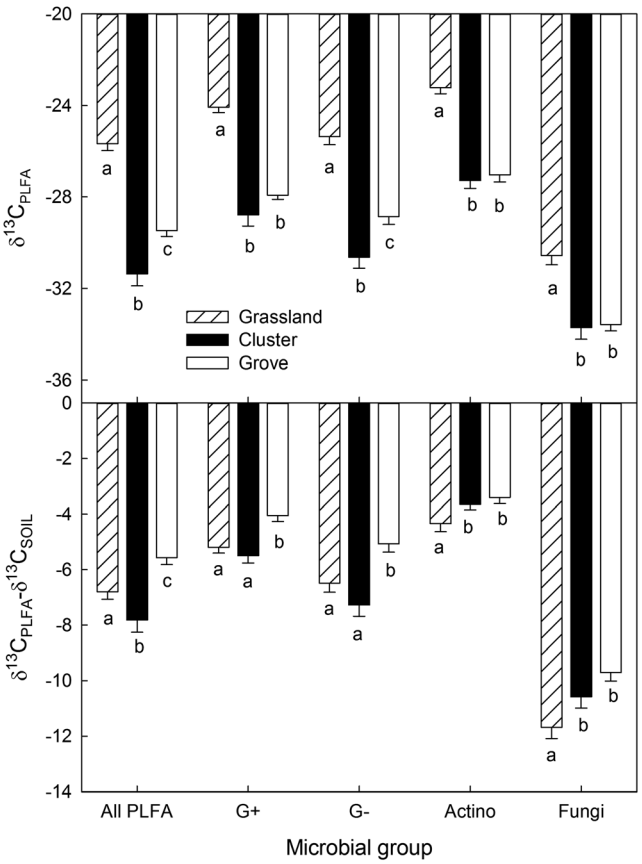

Figure 6. (top) Average $\delta^{13}C$ value of all PLFA and PLFA from microbial groups and (bottom) ^{13}C depletion of PLFA relative to SOC ($\delta^{13}C_{PLFA}$-$\delta^{13}C_{SOIL}$). Values represent means ± standard errors. Letters indicate significant differences between landscape elements.

Reflecting a change in the $\delta^{13}C$ values of SOC with woodland development (Figure 2), there were significant trends between woodland age and the $\delta^{13}C$ values of individual PLFA (Figure 7). This relationship was distinct in the clusters and grove soils for all but fungal and actinobacterial PLFA. In the clusters, the $\delta^{13}C$ values of all PLFAs were significantly ($P < 0.05$) related to stand age using the exponential decay model (equation (1)) with 27–65% of the variation in the $\delta^{13}C$ values explained by stand age. In contrast, in the groves there was a significant relationship between stand age and the $\delta^{13}C$ values for only 7 PLFA, explaining 11–47% of the variation in the data using the exponential decay model (i16:0, a17:0, 16:1ω7c, 18:1ω9c, cy19:0, and 18:0) or the linear model (i/a15:0 and i17:0). Similar to bulk SOC, switching from ^{13}C-enriched to ^{13}C-depleted sources in PLFA was faster in the grove soils but reached a lower $\delta^{13}C$ value in the cluster soils. Generally, PLFA from gram-negative bacteria switched to ^{13}C depleted sources slightly faster (average k of $0.044 \pm 0.005\ year^{-1}$ in clusters and $0.203 \pm 0.031\ year^{-1}$ in groves) than the bulk soil (k of $0.033\ year^{-1}$ in clusters and $0.128\ year^{-1}$ in groves; Figure 2). PLFA from fungi and actinobacteria had the smallest change in $\delta^{13}C$ values across stand age (decreases of 4.0‰ and 4.8‰, respectively, compared to 6.4‰ in SOC across both woodlands) but similar turnover rates as bulk SOC.

4. Discussion

As *Prosopis*-dominated woodlands establish in the grasslands of the Rio Grande Plains, SOC and total N concentrations increase approximately fourfold within 100 years beneath the woody canopies (Figure 1). These findings are broadly consistent with the results of comprehensive reviews of woody encroachment into grasslands around the world showing that most sites with similar or less precipitation than La Copita gain SOC and soil total N in response to encroachment [*Barger et al*., 2011; *Eldridge et al*., 2011] and are similar to prior results at this site [*Archer et al*., 2004; *Liao et al*., 2006b; *Boutton and Liao*, 2010]. The establishment of woody plants also altered the size, composition, and C source of the microbial community. Although some of our hypotheses regarding the response of microbial community composition and C assimilation were confirmed (e.g., increases in gram-negative bacteria), most of the others were not. This suggests that basing changes in microbial community composition and function predominately on a response to increases in chemically complex inputs with woodland encroachment may not be the correct model with which to understand microbial dynamics in this system. However, a decrease in microbial biomass per unit SOC, observed in our study and others (Table 1) [*McCulley et al*., 2004; *Liao and Boutton*, 2008], indicates that increases in C inputs are not supporting a proportional increase in microbial biomass. Relative decreases in microbial-derived amino sugars, relative increases in plant-derived amino acids [*Creamer et al*., 2013a], increases in leaf-derived cutin and root-derived suberin [*Filley et al*., 2008], and slower decomposition of physically

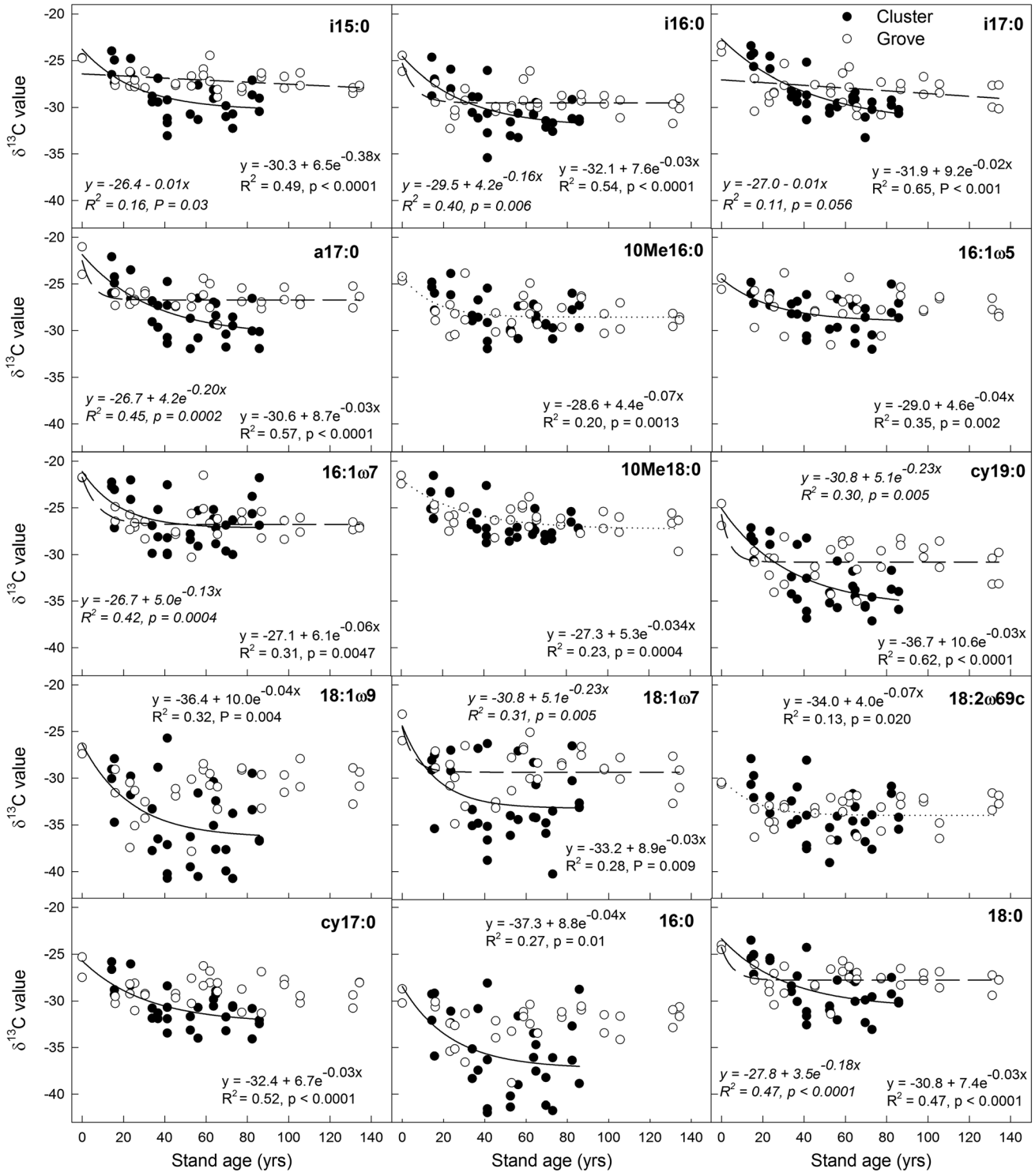

Figure 7. Exponential decay or linear regression models of the $\delta^{13}C$ values of individual PLFA relative to stand age. Cluster fit parameters and trendlines are shown in normal text and solid lines and groves in italics with dashed lines. A dotted line indicates one model fit both cluster and grove soils. A linear regression model was used if it provided a better fit (higher R^2, lower p) then the exponential model. Neither model is shown if $p > 0.05$.

unprotected soil fractions [*Creamer et al*., 2013b], all suggest that at least a portion of the woody plant inputs degrade more slowly than grassland inputs. But contrary to our original hypotheses this does not appear to be the dominant mechanism driving microbial C assimilation.

Compared to the grasslands, the woodland soils had relatively fewer gram-positive bacteria (in October) and actinobacteria, and substantially more gram-negative bacteria. Gram-negative bacteria are typically associated with the rhizosphere and the decomposition of easily degradable substrates (i.e., acting as copiotrophs), while gram-positive bacteria and actinobacteria are typically associated with C limited environments and the decomposition of SOM (i.e., acting as oligotrophs) [*Fierer et al*., 2003; *Treonis et al*., 2004; *Kramer and Gleixner*, 2006; *Bird et al*., 2011]. These functional roles were broadly confirmed in our study by faster switching to woodland C by gram-negative bacteria and by the greater assimilation of ^{13}C-depleted OM in the woodlands by gram-negative bacteria relative to gram-positive bacteria and actinobacteria (Figures 6b and 7). The decrease in oligotrophic biomass and corresponding increase in copiotrophic biomass with woodland development suggests that the microbial community may be responding to overall increases in C inputs, rather than specifically to increases in the more "recalcitrant" compounds. In this system, it appears that the overall increased quantity and availability of inputs [*Hibbard et al*., 2003; *Liao et al*., 2006b], rather than a change "quality" [*Filley et al*., 2008], is the dominant driver of microbial community composition and subsequent OM dynamics with woody encroachment. The observed seasonal differences in microbial community structure within the landscape elements may have resulted from changes in water, carbon, and/or nutrient availability and highlight the importance of multiple samplings to adequately characterize microbial community structure [*Wardle*, 1998].

Interestingly, one gram-negative PLFA (cy19:0) was significantly correlated with woodland age ($R^2 = 0.29$), nearly doubling in relative abundance from the grasslands to the oldest woodlands (Figure 5). Cy19:0 has been shown to increase with decreasing pH [*Bååth and Anderson*, 2003] due to changes in both microbial community composition and in microbial physiology resulting from environmental stressors [*Wixon and Balser*, 2013]. Soil pH under the clusters decreases with progressing woody encroachment (supporting information Figure S3) and decreasing pH is a frequent response to woody encroachment in other regions [*Eldridge et al*., 2011]. Shifts in microbial community composition and physiological state (if driven by pH) may therefore be a common response to the decreases in pH observed with woody encroachment. Alternatively, a change in microbial community structure associated with rhizosphere expansion could also contribute to the increase in cy19:0. In this region the establishment of *P. glandulosa*, and other woody species that colonize beneath its canopy, is associated with substantially higher fine and coarse root biomass [*Hibbard et al*., 2001], and the resulting increase in root-derived material (and presumably root exudation) may have increased the relative abundance of cy19:0. The higher proportions of cy19:0 and gram-negative bacteria could also be due to increases in the symbiotic N_2-fixing bacteria of *P. glandulosa*, as cy19:0 is a common PLFA in Rhizobia, which are N_2 fixing bacteria associated with legumes [*Jarvis and Tighe*, 1994].

In addition to the changes in microbial community composition with woody encroachment, there were changes in the source of assimilated C from grassland C to woodland C. In the woodland soils microbes predominately assimilated the dominant C source (i.e., woodland C), resulting in a relatively constant amount of grassland C remaining with increasing stand age (Figure 3) and despite a lack of grassland inputs. Previous work in this landscape has shown that SOC derived from woody plants accumulates beneath clusters and groves primarily in rapidly cycling physically unprotected soil fractions, with increasing allocation to unprotected soil fractions with stand age [*Liao et al*., 2006b; *Creamer et al*., 2011]. In contrast, SOC derived from grassland vegetation is stored primarily in silt and clay-sized fractions with inherently slower turnover rates [*Liao et al*., 2006a, 2006b]. Thus, microbial assimilation of predominately woodland C in this study, despite the presence of grassland C, was likely driven by its greater accessibility and abundance and resulted in the progressive ^{13}C depletion of PLFA with stand age (Figure 7) as well as the linear relationships with the δ^{13}C values of SOC (supporting information Figure S2). This microbial reliance on accessible woodland C is further supported by long-term laboratory incubations where accessible woodland C was respired to a greater extent than grassland C [*Creamer et al*., 2011].

Between the microbial groups, we observed greater depletion of PLFAs derived from fungi relative to bacteria, due to relatively greater decomposition of ^{13}C-depleted sources (e.g., C_3 forb C in the grasslands or C_3 woody plant C in the woodlands) and/or due to differences in fungal and bacterial metabolism [*Kohl*

et al., 2015]. Among bacteria, gram-positive and actinobacteria were more ^{13}C-enriched than gram-negative bacteria across all landscape elements, suggesting differences in fractionation during lipid biosynthesis [*Hayes*, 2001; *Ruess and Chamberlain*, 2010], preferential decomposition of more microbially processed (and therefore ^{13}C enriched) sources [*Natelhoffer and Fry*, 1988; *Ehleringer et al*., 2000], and/or preferential decomposition of ^{13}C-enriched substrates (such as carbohydrates) [*Hobbie and Werner*, 2004]. When compared to the δ^{13}C value of SOC, the smaller offset of δ^{13}C values of PLFA from fungi in actinobacteria in woodland soils (compared to grassland soils; Figure 6b) and the smaller decrease in δ^{13}C values with stand age (Figure 7) indicate greater microbial utilization of ^{13}C-enriched sources then its abundance in the bulk soil. Woodland soils have proportionately fewer ^{13}C-enriched carbohydrates and amino sugars [*Creamer et al*., 2012], suggesting the ^{13}C enriched source was grassland C. The relative increase in grassland C assimilation by actinobacteria in the woodland soils is consistent with their functional role in degrading both newer plant-derived and older SOM-derived C [*Kramer and Gleixner*, 2006; *Paterson et al*., 2007]. However, this same trend in fungi was unexpected—we predicted this group would preferentially use woodland C. Similarly, our hypothesis that there would be greater fungal biomass in the woodlands relative to the grasslands was not supported (Table 2). Instead of responding to the increases in more complex polymers associated with woody plant inputs, fungi could instead be driven more by an overall increases in substrate quantity due to higher rates of above and belowground productivity associated with shrub encroachment [*Wallenstein et al*., 2007; *Hollister et al*., 2010]. If this is the case, an increase in labile substrates could potentially result in the decomposition of the fine particle associated grassland C (i.e., priming) with woody encroachment [*Montané et al*., 2007], resulting in the slightly ^{13}C enriched values of fungal biomass relative to SOC in the woodlands. This is further supported by demonstrated associations between fungi and priming [*Fontaine et al*., 2011; *Garcia-Pausas and Paterson*, 2011], as well as a potential for the destabilization of mineral-bound grassland C by enhanced root exudation [*Keiluweit et al*., 2015]. However, as fungi and actinobacteria represent a small proportion of the total microbial community at this site (7–8%), they did not impact patterns in total microbial community C assimilation, which were driven by increases in woodland C.

Interestingly, the extent of ^{13}C depletion of PLFA relative to the soil was the smallest in the grove soils (i.e., lower proportional utilization of ^{13}C-depleted sources) and the greatest in the cluster soils (i.e., higher proportional utilization of ^{13}C-depleted sources) with the grasslands intermediate (Figure 6b). A difference in preferential C source utilization between the two woodlands was unexpected, due to the similarities in plant community composition [*Archer et al*., 1988; *Loomis*, 1989], physical fraction distributions and turnover rates [*Liao et al*., 2006a, 2006b], C and N accumulation (Figure 1), and microbial community composition (Figure 4). However, clusters are dominated by increases in belowground biomass and groves by increases in aboveground biomass [*Hibbard*, 1995; *Hibbard et al*., 2001]. Due to the importance of rhizosphere processes on microbial turnover of SOC [*Sulman et al*., 2014], the differences in plant C allocation may have influenced the differences in microbial C utilization. Alternatively, an argillic horizon at 40–60 cm depth under the clusters is absent under the groves, and these differences in subsoil clay content may be altering C processes in the upper soil horizons. However, these slight preferences for grassland C (in groves) and woodland C (in clusters) by the microbial communities has not translated into changes in C or N accumulation (Figures 1 and 3), likely because the overall C source utilization patterns of the groups remained consistent (Figure 6).

In other regions where woodland encroachment is not accompanied by increases in primary productivity of the invading plants or by increases in SOM accessibility, C source utilization patterns of the microbial community may be more responsive to the chemistry of the inputs, as the available pool of easily degradable and available substrates may be smaller. Moreover, there could be more extensive degradation of the remaining grassland C resulting in overall C losses, which instead remained relatively stable with woodland encroachment in this system. In addition to the changes in productivity between the native and invading plants, changes in OM accessibility can alter microbial community composition and function and consequently C cycling.

5. Conclusions

Grassland to woodland transitions are often accompanied by changes in primary production and input chemistry, with consequences for soil C and N storage and dynamics. In the Rio Grande Plains region of Texas, shrub encroachment has increased soil C and N concentrations, the quantity of plant inputs, the

allocation of C to physical fractions, and the C chemistry within physically unprotected soil fractions. As a result, microbial community composition and activity was altered. Most notably, the gram-negative bacteria cy19:0 increased in abundance linearly with time following the establishment of woody plants in grassland. With increases in the amount and availability of woodland C, soil microorganisms in the wooded areas predominately utilized this more physically accessible C, despite a relatively constant amount of grassland C. There were also differences between the two woodland systems, where compared to the remnant grassland soils, microbes in the clusters utilized a greater proportion of woodland C, while microbes in the groves utilized a greater proportion of grassland C. These differences may result from the source of C inputs or differences in subsoil clay content in the two woodlands, although this has not translated into differences in C and N storage.

Acknowledgments

This work was supported by the NSF Biogeosciences Program (EAR-0525349), a Purdue Climate Change Research Center seed grant to T.R.F., and by the USDA National Institute of Food and Agriculture (Hatch Project 1003961 to T.W.B.). All data used in this publication can be found in the supporting information. Thanks to Ron Turco and Marianne Bischoff for training on PLFA quantification and extraction and to Ian Schaller for help with PLFA extraction. We also thank two anonymous reviewers who greatly improved the manuscript.

References

Amelung, W., S. Brodowski, A. Sandhage-Hofmann, and R. Bol (2008), Chapter 6: Combining biomarker with stable isotope analyses for assessing the transformation and turnover of soil organic matter, in *Advances in Agronomy*, vol. 100, edited by D. L. Sparks, pp. 155–250, Academic Press, Burlington.

Archer, S. R. (1990), Development and stability of grass/woody mosaics in a subtropical savanna parkland, Texas, U.S.A., *J. Biogeogr.*, *17*(4/5), 453–462, doi:10.2307/2845377.

Archer, S. R., C. J. Scifres, C. R. Bassham, and R. Maggio (1988), Autogenic succession in a subtropical savanna: Conversion of grassland to thorn woodland, *Ecol. Monogr.*, *58*, 111–127.

Archer, S. R., D. S. Schimel, and E. A. Holland (1995), Mechanisms of shrubland expansion: Land use, climate or CO_2?, *Clim. Change*, *29*(1), 91–99, doi:10.1007/BF01091640.

Archer, S. R., T. W. Boutton, and K. A. Hibbard (2001), Trees in grasslands: Biogeochemical consequences of woody plant expansion, in *Global Biogeochemical Cycles in the Climate System*, edited by E.-D. Schulze et al., pp. 1–46, Academic Press, San Diego, Calif.

Archer, S. R., T. W. Boutton, and C. R. McMurtry (2004), Carbon and nitrogen accumulation in a savanna landscape: Field and modeling perspectives, in *Global Environmental Change in the Ocean and on Land*, edited by M. Shiyomi, pp. 359–373, TERRAPUB, Tokyo.

Bååth, E., and T.-H. Anderson (2003), Comparison of soil fungal/bacterial ratios in a pH gradient using physiological and PLFA-based techniques, *Soil Biol. Biochem.*, *35*(7), 955–963, doi:10.1016/S0038-0717(03)00154-8.

Bai, E., T. W. Boutton, X. B. Wu, F. Liu, and S. R. Archer (2009), Landscape-scale vegetation dynamics inferred from spatial patterns of soil $\delta^{13}C$ in a subtropical savanna parkland, *J. Geophys. Res.*, *114*, G01019, doi:10.1029/2008JG000839.

Bai, E., T. W. Boutton, F. Liu, X. Ben Wu, and S. R. Archer (2012), Spatial patterns of soil $\delta^{13}C$ reveal grassland-to-woodland successional processes, *Org. Geochem.*, *42*(12), 1512–1518, doi:10.1016/j.orggeochem.2010.11.004.

Balesdent, J., and A. Mariotti (1996), Measurement of soil organic matter turnover using 13C natural abundance, in *Mass Spectrometry of Soils*, vol. 41, edited by T. W. Boutton and S.-I. Yamasaki, pp. 83–111, Marcel Dekker, New York.

Barger, N. N., S. R. Archer, J. L. Campbell, C. Huang, J. A. Morton, and A. K. Knapp (2011), Woody plant proliferation in North American drylands: A synthesis of impacts on ecosystem carbon balance, *J. Geophys. Res.*, *116*, G00K07, doi:10.1029/2010JG001506.

Bird, J. A., D. J. Herman, and M. K. Firestone (2011), Rhizosphere priming of soil organic matter by bacterial groups in a grassland soil, *Soil Biol. Biochem.*, *43*(4), 718–725, doi:10.1016/j.soilbio.2010.08.010.

Blanchette, R. A. (1991), Delignification by wood-decay fungi, *Annu. Rev. Phytopathol.*, *29*, 381–403.

Blaser, W. J., G. K. Shanungu, P. J. Edwards, and H. Olde Venterink (2014), Woody encroachment reduces nutrient limitation and promotes soil carbon sequestration, *Ecol. Evol.*, *4*(8), 1423–1438, doi:10.1002/ece3.1024.

Bligh, E. G., and W. J. Dyer (1959), A rapid method of total lipid extraction and purification, *Can. J. Biochem. Physiol.*, *37*(8), 911–917.

Bond, W. J., and G. F. Midgley (2000), A proposed CO_2-controlled mechanism of woody plant invasion in grasslands and savannas, *Global Change Biol.*, *6*(8), 865–869, doi:10.1046/j.1365-2486.2000.00365.x.

Boutton, T. W., and J. D. Liao (2010), Changes in soil nitrogen storage and $\delta^{15}N$ with woody plant encroachment in a subtropical savanna parkland landscape, *J. Geophys. Res.*, *115*, G03019, doi:10.1029/2009JG001184.

Boutton, T. W., S. R. Archer, A. J. Midwood, S. F. Zitzer, and R. Bol (1998), $\delta^{13}C$ values of soil organic carbon and their use in documenting vegetation change in a subtropical savanna ecosystem, *Geoderma*, *82*(1–3), 5–41, doi:10.1016/S0016-7061(97)00095-5.

Boutton, T. W., J. D. Liao, T. R. Filley, and S. R. Archer (2009), Belowground carbon storage and dynamics accompanying woody plant encroachment in a subtropical savanna, in *Soil Carbon Sequestration and the Greenhouse Effect*, edited by R. Lal and R. F. Follett, pp. 181–205, Soil Sci. Soc. of Am., Madison, WI.

Brant, J. B., E. W. Sulzman, and D. D. Myrold (2006), Microbial community utilization of added carbon substrates in response to long-term carbon input manipulation, *Soil Biol. Biochem.*, *38*(8), 2219–2232, doi:10.1016/j.soilbio.2006.01.022.

Brewer, E. A. (2010), Response of soil microbial communities and nitrogen cycling processes to changes in vegetation input, Oregon State Univ., PhD dissertation.

Butler, J. L., M. A. Williams, P. J. Bottomley, and D. D. Myrold (2003), Microbial community dynamics associated with rhizosphere carbon flow, *Appl. Environ. Microbiol.*, *69*(11), 6793–6800, doi:10.1128/AEM.69.11.6793-6800.2003.

Coplen, T. B. (2011), Guidelines and recommended terms for expression of stable-isotope-ratio and gas-ratio measurement results, *Rapid Commun. Mass Spectrom.*, *25*(17), 2538–2560, doi:10.1002/rcm.5129.

Creamer, C. A., T. R. Filley, T. W. Boutton, S. Oleynik, and I. B. Kantola (2011), Controls on soil carbon accumulation during woody plant encroachment: Evidence from physical fractionation, soil respiration, and $\delta^{13}C$ of respired CO_2, *Soil Biol. Biochem.*, *43*(8), 1678–1687, doi:10.1016/j.soilbio.2011.04.013.

Creamer, C. A., T. R. Filley, D. C. Olk, A. Plante, C. Peltre, S. M. Top, and T. W. Boutton (2012), Degree of woody encroachment into grasslands controls soil carbohydrate and amino compound changes during long term laboratory incubation, *Org. Geochem.*, *52*, 23–31, doi:10.1016/j.orggeochem.2012.08.005.

Creamer, C. A., T. R. Filley, D. C. Olk, D. E. Stott, V. Dooling, and T. W. Boutton (2013a), Changes to soil organic N dynamics with leguminous woody plant encroachment into grasslands, *Biogeochemistry*, *113*(1–3), 307–321, doi:10.1007/s10533-012-9757-5.

Creamer, C. A., T. R. Filley, and T. W. Boutton (2013b), Long-term incubations of size and density separated soil fractions to inform soil organic carbon decay dynamics, *Soil Biol. Biochem.*, *57*, 496–503, doi:10.1016/j.soilbio.2012.09.007.
de Graaff, M.-A., H. L. Throop, P. S. J. Verburg, J. A. A. Iii, and X. Campos (2014), A synthesis of climate and vegetation cover effects on biogeochemical cycling in shrub-dominated drylands, *Ecosystems*, 1–15, doi:10.1007/s10021-014-9764-6.
Ehleringer, J. R., N. Buchmann, and L. B. Flanagan (2000), Carbon isotope ratios in belowground carbon cycle processes, *Ecol. Appl.*, *10*(2), 412–422, doi:10.1890/1051-0761(2000)010[0412:CIRIBC]2.0.CO;2.
Eldridge, D. J., M. A. Bowker, F. T. Maestre, E. Roger, J. F. Reynolds, and W. G. Whitford (2011), Impacts of shrub encroachment on ecosystem structure and functioning: Towards a global synthesis, *Ecol. Lett.*, *14*(7), 709–722, doi:10.1111/j.1461-0248.2011.01630.x.
Fierer, N., J. P. Schimel, and P. A. Holden (2003), Variations in microbial community composition through two soil depth profiles, *Soil Biol. Biochem.*, *35*(1), 167–176, doi:10.1016/S0038-0717(02)00251-1.
Filley, T. R., T. W. Boutton, J. D. Liao, J. D. Jastrow, and D. E. Gamblin (2008), Chemical changes to nonaggregated particulate soil organic matter following grassland-to-woodland transition in a subtropical savanna, *J. Geophys. Res.*, *113*, G03009, doi:10.1029/2007JG000564.
Findlay, R. H., G. M. King, and L. Watling (1989), Efficacy of phospholipid analysis in determining microbial biomass in sediments, *Appl. Environ. Microbiol.*, *55*(11), 2888–2893.
Fontaine, S., C. Henault, A. Aamor, N. Bdioui, J. M. G. Bloor, V. Maire, B. Mary, S. Revaillot, and P. A. Maron (2011), Fungi mediate long term sequestration of carbon and nitrogen in soil through their priming effect, *Soil Biol. Biochem.*, *43*(1), 86–96, doi:10.1016/j.soilbio.2010.09.017.
Frostegård, Å., A. Tunlid, and E. Bååth (1991), Microbial biomass measured as total lipid phosphate in soils of different organic content, *J. Microbiol. Methods*, *14*(3), 151–163, doi:10.1016/0167-7012(91)90018-L.
Garcia-Pausas, J., and E. Paterson (2011), Microbial community abundance and structure are determinants of soil organic matter mineralisation in the presence of labile carbon, *Soil Biol. Biochem.*, *43*(8), 1705–1713, doi:10.1016/j.soilbio.2011.04.016.
Hayes, J. M. (2001), Fractionation of carbon and hydrogen isotopes in biosynthetic processes, *Rev. Mineral. Geochem.*, *43*(1), 225–277, doi:10.2138/gsrmg.43.1.225.
Hibbard, K. A. (1995), Landscape patterns of carbon and nitrogen dynamics in a subtropical savanna: Observations and models, PhD Dissertation, Texas A&M Univ., College Station, Tex.
Hibbard, K. A., S. Archer, D. S. Schimel, and D. W. Valentine (2001), Biogeochemical changes accompanying woody plant encroachment in a subtropical savanna, *Ecology*, *82*(7), 1999–2011.
Hibbard, K. A., D. S. Schimel, S. R. Archer, D. S. Ojima, and W. Parton (2003), Grassland to woodland transitions: Integrating changes in landscape structure and biogeochemistry, *Ecol. Appl.*, *13*(4), 911–926.
Hobbie, E. A., and R. A. Werner (2004), Intramolecular, compound-specific, and bulk carbon isotope patterns in C_3 and C_4 plants: A review and synthesis, *New Phytol.*, *161*(2), 371–385, doi:10.2307/1514321.
Hollister, E. B., C. W. Schadt, A. V. Palumbo, R. James Ansley, and T. W. Boutton (2010), Structural and functional diversity of soil bacterial and fungal communities following woody plant encroachment in the southern Great Plains, *Soil Biol. Biochem.*, *42*(10), 1816–1824, doi:10.1016/j.soilbio.2010.06.022.
Jackson, R. B., J. L. Banner, E. G. Jobbagy, W. T. Pockman, and D. H. Wall (2002), Ecosystem carbon loss with woody plant invasion of grasslands, *Nature*, *418*(6898), 623–626, doi:10.1038/nature00910.
Jarvis, B. D. W., and S. W. Tighe (1994), Rapid identification of Rhizobium species based on cellular fatty acid analysis, *Plant Soil*, *161*(1), 31–41, doi:10.1007/BF02183083.
Kantola, I. B. (2012), Biogeochemistry of woody plant invasion: Phosphorus cycling and microbial community composition, PhD Dissertation, Texas A&M Univ., College Station, Tex.
Keiluweit, M., J. J. Bougoure, P. S. Nico, J. Pett-Ridge, P. K. Weber, and M. Kleber (2015), Mineral protection of soil carbon counteracted by root exudates, *Nat. Clim. Change*, *5*(6), 588–595, doi:10.1038/nclimate2580.
Knapp, A. K., et al. (2008), Shrub encroachment in North American grasslands: Shifts in growth form dominance rapidly alters control of ecosystem carbon inputs, *Global Change Biol.*, *14*(3), 615–623, doi:10.1111/j.1365-2486.2007.01512.x.
Kohl, L., J. Laganière, K. A. Edwards, S. A. Billings, P. L. Morrill, G. V. Biesen, and S. E. Ziegler (2015), Distinct fungal and bacterial $\delta^{13}C$ signatures as potential drivers of increasing $\delta^{13}C$ of soil organic matter with depth, *Biogeochemistry*, *124*(1–3), 13–26, doi:10.1007/s10533-015-0107-2.
Kramer, C., and G. Gleixner (2006), Variable use of plant- and soil-derived carbon by microorganisms in agricultural soils, *Soil Biol. Biochem.*, *38*(11), 3267–3278, doi:10.1016/j.soilbio.2006.04.006.
Kramer, C., and G. Gleixner (2008), Soil organic matter in soil depth profiles: Distinct carbon preferences of microbial groups during carbon transformation, *Soil Biol. Biochem.*, *40*(2), 425–433, doi:10.1016/j.soilbio.2007.09.016.
Liao, J. D., and T. W. Boutton (2008), Soil microbial biomass response to woody plant invasion of grassland, *Soil Biol. Biochem.*, *40*(5), 1207–1216, doi:10.1016/j.soilbio.2007.12.018.
Liao, J. D., T. W. Boutton, and J. D. Jastrow (2006a), Organic matter turnover in soil physical fractions following woody plant invasion of grassland: Evidence from natural ^{13}C and ^{15}N, *Soil Biol. Biochem.*, *38*(11), 3197–3210, doi:10.1016/j.soilbio.2006.04.004.
Liao, J. D., T. W. Boutton, and J. D. Jastrow (2006b), Storage and dynamics of carbon and nitrogen in soil physical fractions following woody plant invasion of grassland, *Soil Biol. Biochem.*, *38*(11), 3184–3196, doi:10.1016/j.soilbio.2006.04.003.
Loomis, L. E. (1989), Influence of hetergenous subsoil development on vegetation patterns in a subtropical savanna parkland, Texas, PhD Dissertation, Texas A&M Univ., College Station, Tex.
McCulley, R. L., S. R. Archer, T. W. Boutton, F. M. Hons, and D. A. Zuberer (2004), Soil respiration and nutrient cycling in wooded communities developing in grassland, *Ecology*, *85*(10), 2804–2817.
Montané, F., P. Rovira, and P. Casals (2007), Shrub encroachment into mesic mountain grasslands in the Iberian peninsula: Effects of plant quality and temperature on soil C and N stocks, *Global Biogeochem. Cycles*, *21*, GB4016, doi:10.1029/2006GB002853.
Natelhoffer, K. J., and B. Fry (1988), Controls on natural nitrogen-15 and carbon-13 abundances in forest soil organic matter, *Soil Sci. Soc. Am. J.*, *52*(6), 1633, doi:10.2136/sssaj1988.03615995005200060024x.
Pacala, S. W., et al. (2001), Consistent land- and atmosphere-based U.S. carbon sink estimates, *Science*, *292*(5525), 2316–2320, doi:10.1126/science.1057320.
Paterson, E., T. Gebbing, C. Abel, A. Sim, and G. Telfer (2007), Rhizodeposition shapes rhizosphere microbial community structure in organic soil, *New Phytol.*, *173*, 600–610.
Ruess, L., and P. M. Chamberlain (2010), The fat that matters: Soil food web analysis using fatty acids and their carbon stable isotope signature, *Soil Biol. Biochem.*, *42*(11), 1898–1910, doi:10.1016/j.soilbio.2010.07.020.

Saintilan, N., and K. Rogers (2015), Woody plant encroachment of grasslands: A comparison of terrestrial and wetland settings, *New Phytol.*, *205*(3), 1062–1070, doi:10.1111/nph.13147.

Scholes, R. J., and S. R. Archer (1997), Tree-grass interactions in savannas, *Annu. Rev. Ecol. Syst.*, *28*, 517–544.

Stoker, R. L. (1997), Object-oriented, spatially explicit simulation model of vegetation dynamics in a south Texas savanna, PhD Dissertation, Texas A&M Univ., College Station, Tex.

Sulman, B. N., R. P. Phillips, A. C. Oishi, E. Shevliakova, and S. W. Pacala (2014), Microbe-driven turnover offsets mineral-mediated storage of soil carbon under elevated CO_2, *Nat. Clim. Change*, *4*, 1099–1102.

Tavi, N. M., P. J. Martikainen, K. Lokko, M. Kontro, B. Wild, A. Richter, and C. Biasi (2013), Linking microbial community structure and allocation of plant-derived carbon in an organic agricultural soil using $^{13}CO_2$ pulse-chase labelling combined with ^{13}C-PLFA profiling, *Soil Biol. Biochem.*, *58*, 207–215, doi:10.1016/j.soilbio.2012.11.013.

Treonis, A. M., N. J. Ostle, A. W. Stott, R. Primrose, S. J. Grayston, and P. Ineson (2004), Identification of groups of metabolically-active rhizosphere microorganisms by stable isotope probing of PLFAs, *Soil Biol. Biochem.*, *36*(3), 533–537, doi:10.1016/j.soilbio.2003.10.015.

Wallenstein, M. D., S. McMahon, and J. Schimel (2007), Bacterial and fungal community structure in Arctic tundra tussock and shrub soils, *FEMS Microbiol. Ecol.*, *59*(2), 428–435, doi:10.1111/j.1574-6941.2006.00260.x.

Wardle, D. A. (1998), Controls of temporal variability of the soil microbial biomass: A global-scale synthesis, *Soil Biol. Biochem.*, *30*(13), 1627–1637, doi:10.1016/S0038-0717(97)00201-0.

White, D. C., W. M. Davis, J. S. Nickels, J. D. King, and R. J. Bobbie (1979), Determination of the sedimentary microbial biomass by extractible lipid phosphate, *Oecologia*, *40*, 51–62.

Wixon, D. L., and T. C. Balser (2013), Toward conceptual clarity: PLFA in warmed soils, *Soil Biol. Biochem.*, *57*, 769–774, doi:10.1016/j.soilbio.2012.08.016.

Journal of Geophysical Research: Biogeosciences

Supporting Information for

Grassland to woodland transitions: dynamic response of microbial community structure and carbon use patterns

Courtney A Creamer[1*†], Timothy R Filley[1], Thomas W Boutton[2], Helen I Rowe[3,4]

[1]Dept of Earth, Atmospheric, and Planetary Sciences, and the Purdue Climate Change Research Center, Purdue University, West Lafayette IN 47907

[2]Dept of Ecosystem Science and Management, Texas A&M University, College Station, TX 77843

[3]McDowell Sonoran Conservancy, Scottsdale, AZ, 85254

[4]School of Life Sciences and Julie Ann Wrigley Global Institute of Sustainability, Arizona State University, Tempe, AZ 85287

†Current address: US Geological Survey, 345 Middlefield Rd, Menlo Park CA 94025

Contents of this file

Additional Supporting Information (Files uploaded separately)

Introduction

The supporting information in this file provides additional text, figures, and data associated with the publication. The supplemental text provides information on the extraction and collection conditions for gas chromatography-mass spectrometry (GC-MS) and gas chromatography-combustion-isotope ratio mass spectrometry (GC-c-IRMS) analysis of microbial PLFAs. The supporting figures show linear relationships between woodland stand age and the relative abundance (mol %) of individual phospholipids and the $\delta^{13}C$ values of individual phospholipids relative to the $\delta^{13}C$ values of soil C. The datasets contain relevant data for all figures and tables in the manuscript, primarily the concentration and $\delta^{13}C$ values of soil C and the relative abundance and $\delta^{13}C$ values of individual phospholipids. Data is provided for all 15 sites sampled at each of the three landscape elements across the two sampling seasons (total of 90 samples). Associated ages are also provided.

Text S1:

PLFA extraction and FAME derivatization

Between 5 – 8 g of freeze-dried soil was weighed into glass screw cap tubes with Teflon lined caps. A recovery standard (15 µg of 1,2-dinonadecanoyl-*sn*-glycero-3-phosphocholine, Avanti Polar Lipids, Alabaster, AL) was added to the soil along with 30

mL of chloroform, methanol, and phosphate buffer (50 mM, pH 7.0) in a 1:2:0.8 ratio. Tubes were vigorously shaken for 30 seconds, wrapped in aluminum foil, and kept at 4 °C for 24 hrs for lipid extraction. An additional 8 mL chloroform and 8 mL distilled water (stored over chloroform) was added to the tubes to aid in phase separation. The tubes were shaken vigorously for 30 seconds and allowed to settle overnight (16 – 24 hrs) while wrapped in aluminum foil at 4 °C. Once the phases were completely separated, the top (aqueous) phase was aspirated and discarded while the bottom (organic) phase containing extracted lipids was filtered into a clean pear-shaped flask through glass wool packed glass funnels. The organic phase was reduced to approximately 1 mL with a rotary evaporator and blown dry with N_2 gas. Solid phase extraction (SPE) columns were prepared by baking 200 mg of silicic acid in glass columns with a quartz wool plug at 450 °C for 4 hr and stored at 105 °C until use. Columns were placed in a Visiprep™ SPE vacuum manifold (Supleco, Bellefonte, PA) and washed and conditioned with 4 mL methanol followed by 4 mL chloroform. Samples were re-suspended in 1 mL of 2 % methanol in chloroform and quantitatively transferred to the SPE columns. Neutral lipids were eluted with 4 mL chloroform and glycolipids with 4 mL acetone; both fractions were discarded. The column drained completely between solvents but did not dry. Phospholipids were eluted with 4 mL methanol, dried under N_2 gas, and stored at -20 °C.

Phospholipids were suspended in exactly 1.0 mL of chloroform; 100 µL was transferred to a 4 mL vial for quantitative GC-MS, 100 µL to a 2 mL glass ampoule for total biomass determination, and the remaining 800 µL was used for GC-c-IRMS. All splits were dried under N_2 gas and stored at -20 °C. Phospholipid splits for derivatization were re-suspended in 250 µL methanol, 250 µL toluene, and 500 µL methanolic KOH (0.50 M), capped securely, and placed in a heating block (45 min at 37 °C). After cooling to room temperature, 900 µL hexane, 100 µL 1M acetic acid, and 1 mL 18 MΩ water (stored over chloroform) was added to the vials and vortexed for 20 seconds. After settling, the top layer was removed and transferred to a clean 4 mL vial. This hexane extraction (900 µL) was repeated three times and none of the lower phase was transferred. The hexane was evaporated to near dryness with N_2 gas. Samples were re-suspended in 25 µL of the internal standard (methyl decanoate, Sigma-Aldrich, St. Louis, MO) and 25 µL hexane for quantitative GC-MS, or in 44 µL hexane and 6 µL of the isotopic standard (tetradecane C14 *n*-alkane [at 145 ng μL^{-1}], Biochemical Labs at Indiana University, Bloomington, IN) for GC-c-IRMS. Samples were analyzed within 24 hrs of derivatization (samples were stored at -20 °C until analysis if necessary). Twenty percent of the samples were extracted, derivatized, and analyzed in duplicate. Duplicate averages are presented where applicable.

FAME quantification

The 100 µL aliquots of PLFA extracts (10 % of the PLFA extract) were dried under a stream of N_2 and subjected to mild alkaline methanolysis to form FAMEs (described above). The FAMEs were analyzed by GC-MS on a Shimadzu QP2010+ (Shimadzu, Kyoto, Japan) with a 60 m Rtx-5 column (Restek, Bellefonte, PA) and the following GC oven program: 50-180 °C at 8 °C min^{-1}, 180-250 °C at 2.5 °C min^{-1}, 250-280 °C at 8 °C min^{-1}, hold 10 minutes, for a total runtime of 58 minutes. The sample was injected in splitless injection mode at 280 °C with a 1.00 minute sampling time and a column flow of 1.00 mL min^{-1} The GC-MS was operated in selected-ion-monitoring (SIM)/scan mode to improve sensitivity and the detector was at 280 °C. Scan mode monitored from m/z 44-550 and ions used for SIM were based upon fragmentation patterns. Due to similarities in ion fragmentation patterns, compounds with the same molecular weight and similar structures (*e.g.* iso- and antiso- branching) were identified

primarily based upon retention time and by comparison to a 26 component bacterial acid methyl ester mix (Matreya Inc, Pleasant Gap, PA, Sulpelco, Bellefonte, PA). FAMEs were quantified using a 6-point calibration curve of the 26 component standard and the internal recovery standard, methyl decanoate (Sigma-Aldrich, St. Louis, MO), added to samples just prior to quantification. 1,2-dinonadecanoyl-*sn*-glycero-3-phosphocholine (19:0 phospholipid, Avanti Polar Lipids, Alabaster, AL) was added to the soil to monitor extraction efficiency and the efficiency of methylation (recoveries varied from 70 – 102 % with an average of 93 %). Twenty-one FAMEs were identified and quantified, and are named by shorthand notation, where the number of carbon atoms is given, followed by the number of unsaturated bonds and the location of the unsaturated bonds from the methyl (ω) end of the fatty acid. The letters *c* and *t* represent *cis* and *trans* isomers of unsaturated FAMEs, *a* and *i* represent *anteiso-* and *iso-* branching of saturated FAMEs, and the prefix *cy-* signifies cyclopropyl fatty acids. Unknown branching positions on saturated fatty acids are given by the prefix *br-* and known methyl branching positions on saturated fatty acids are given by their position relative to the carboxyl end. PLFAs were separated into the following groups: fungi = 18:2ω6,9c; gram-negative bacteria: 16:1ω7, cy17:0, 18:1ω7, 18:1ω9, cy19:0; gram-positive bacteria: i15:0, a15:0, i16:0, i17:0, a17:0; actinobacteria: 10Me16:0, 10Me18:0. Ratios of fungi to bacteria (F:B) were calculated as the ratio of 18:2ω6,9c to the sum of gram-positive, gram-negative, and actinobacteria PLFAs.

Isotopic composition of FAMEs

A split of the extracted PLFAs (80 %) was subjected to mild alkaline methanolysis to form FAMEs (as described above) and analyzed for their $\delta^{13}C$ values using GC-c-IRMS with a cooled injection system (CIS 4, Gerstel, Mülheim adRuhr, Germany) interfaced to a 6890A GC (Agilent/HP, Palo Alto, CA), a combustion column held at 950°C, and a PDZ Europa 20/22 IRMS (Sercon, Crewe, UK). Individual FAMEs were identified based upon retention times, as determined on the Shimadzu QP2010+ GC-MS. Of the 21 FAMEs identified on the QP2010+, one was below detection (15:0), and 4 FAMEs were co-eluted to form two groups (i15:0 + a15:0, 17:0 + 10Me17:0). The $\delta^{13}C$ value obtained for the two co-eluted gram-positive biomarkers was included in the gram-positive group in subsequent analyses, while 10Me17:0 and 17:0 were omitted from the actinobacteria and general microbial groupings, respectively. The CIS injection port was operated in solvent vent mode with splitless transfer and 1-2 µL injections. During solvent venting the injection port was held at 25 °C with a vent pressure of 5.0 psi and vent flow of 100 mL min^{-1}. After a vent time of 0.08 min the column flow was increased to 1.0 mL min^{-1}, and for splitless transfer at 0.14 min the injection port temperature was ramped to 280 °C at 12 °C s^{-1} with a sampling time of 1.5 min and purge flow of 50 mL min^{-1}. The 6890A GC interfaced to the 20/22 IRMS also used a 60 m Rtx-5 column, but with a slightly slower temperature ramp to improve baseline separation of 18:2ω6,9c, 18:1ω9, and 18:1ω7: 50-150 °C at 10 °C min^{-1}, 150-250°C at 2.5°C min^{-1}, 200-230 °C at 1.25 °C min^{-1}, 230-280 °C at 10 °C min^{-1}, hold 2 min at 280 °C. Duplicate injections for each sample were averaged. Across all samples, the average $\delta^{13}C$ value of the *n*-alkane isotopic standard (actual $\delta^{13}C$ value = - 30.66 ‰) was -31.0 ± 1.2 ‰. Once a week a calibration curve (5 levels, 7 – 56 ng μL^{-1}) of an isotopically verified n-alkane mix (n-alkane mixture C3, Indiana University) was run to ensure minimum isotopic drift across concentration and run duration.

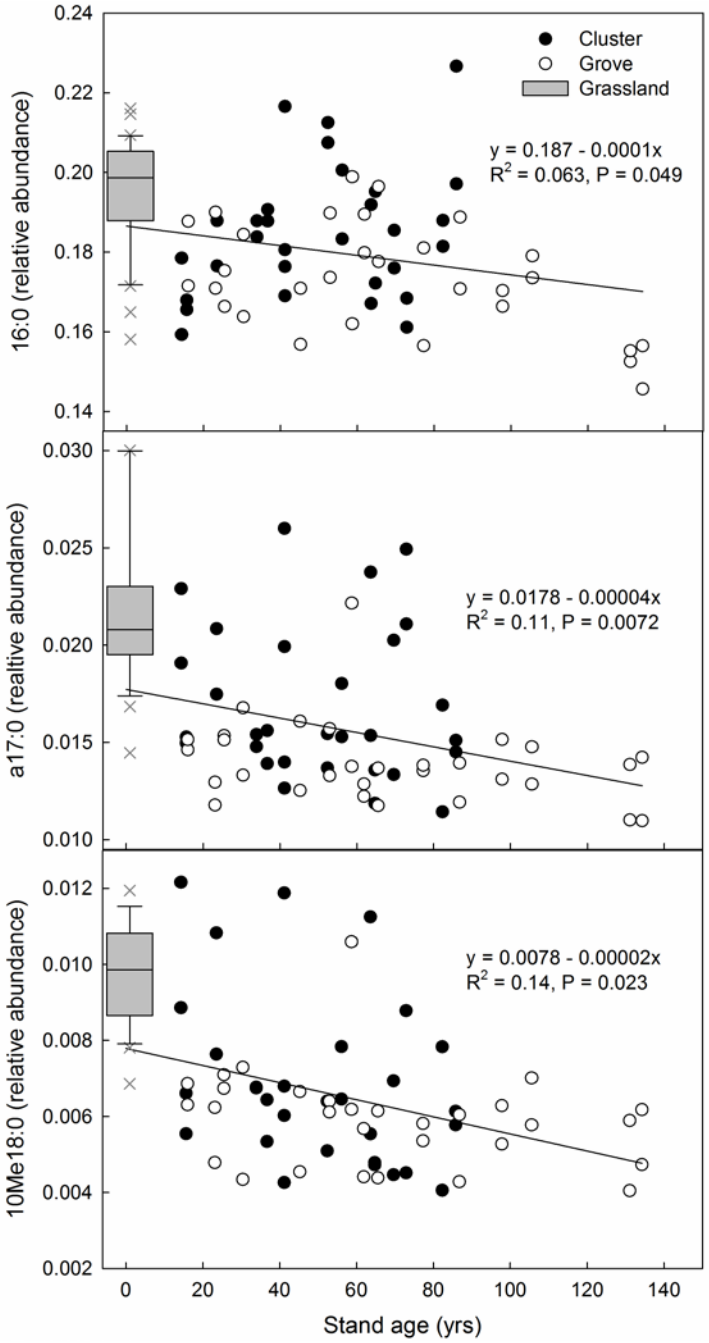

Figure S1. Linear regressions of 16:0 (top), a17:0 (middle), and 10Me18:0 (bottom), relative to stand age. Grassland soils are represented by a boxplot at time 0 with the whiskers at the 10th and 90th percentiles (boxplot outliers shown as an X).

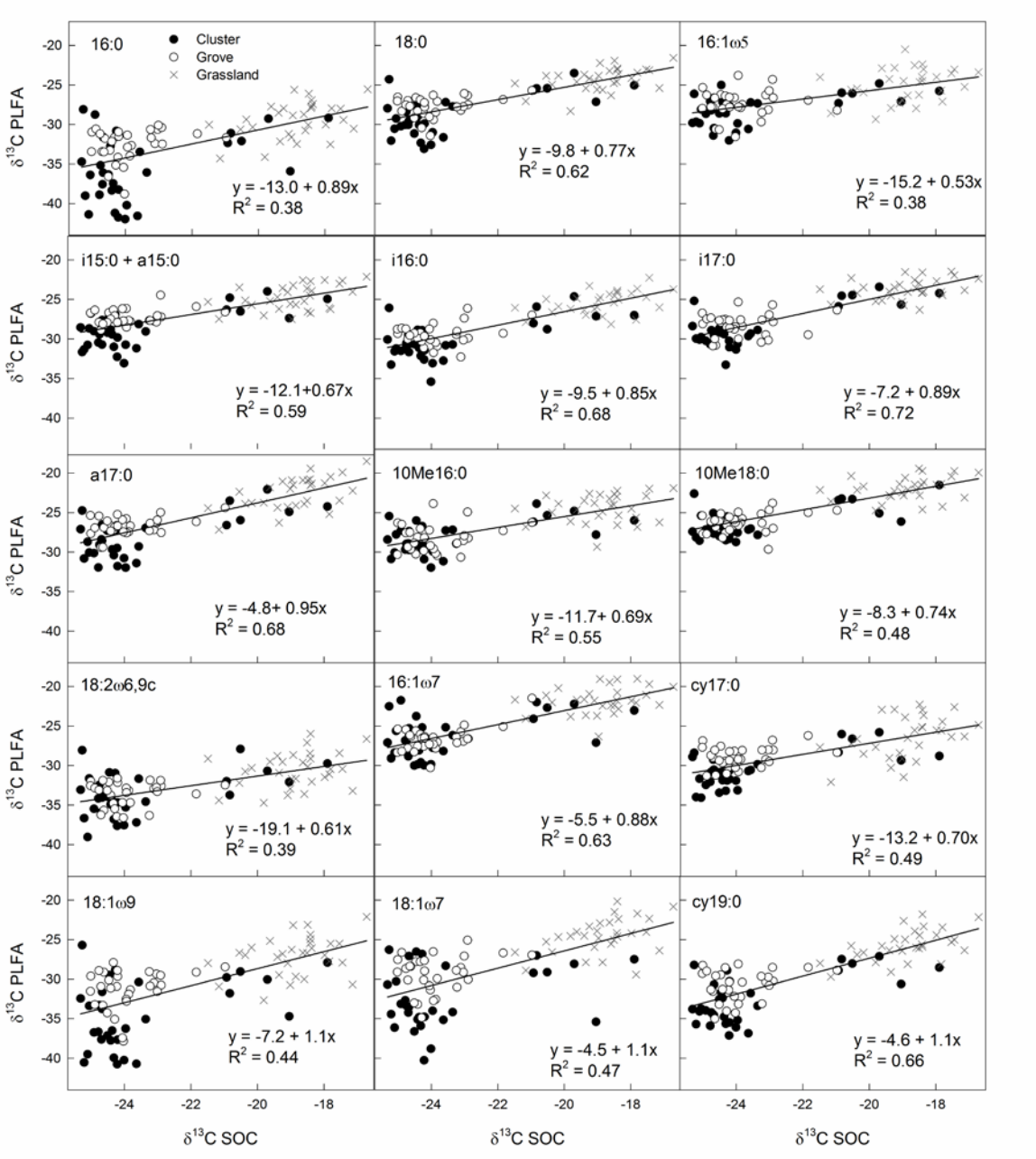

141

142 **Figure S2.** Linear regressions of the $\delta^{13}C$ values of PLFAs relative to the $\delta^{13}C$ values of
143 SOC across all landscape elements. Each panel shows a different PLFA regression,
144 and symbols indicate different landscape elements. Regression equations are shown.
145 All regressions are significant at $P < 0.001$.

146

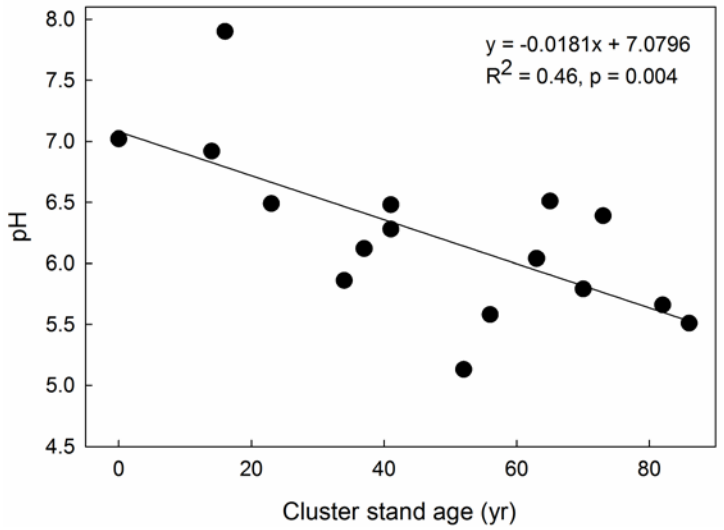

Figure S3. pH in relation to cluster age (yrs) from the 0-5 cm depth. Data for the groves was collected.

Data Set S1. This dataset contains information on the C and N concentration, soil $\delta^{13}C$ values, fraction (0-1) of grassland-derived C, and microbial biomass yields for all fifteen sites with associated ages along the chronosequence, within each of the three landscape elements (grass, cluster, grove), across the two sampling seasons (May, Oct).

Data Set S2. This dataset contains the relative abundances (mol %) of all identified microbial phospholipids for the fifteen sites along the chronosequence within each of the three landscape elements (grass, cluster, grove) and across the two sampling seasons (May, Oct).

Data Set S3. This dataset contains the individual $\delta^{13}C$ values of all identified microbial phospholipids and the associated $\delta^{13}C$ values of soil carbon for all fifteen sites with associated ages along the chronosequence within each of the three landscape elements (grass, cluster, grove) and across the two sampling seasons (May, Oct).

Data Set S4. This dataset contains the average $\delta^{13}C$ values of total microbial biomass and microbial groups for all fifteen sites with associated ages along the chronosequence within each of the three landscape elements (grass, cluster, grove) and across the two sampling seasons (May, Oct).